Vol 466|5 August 2010|doi:10.1038/nature09301

LETTERS

Branched tricarboxylic acid metabolism in *Plasmodium falciparum*

Kellen L. Olszewski[1], Michael W. Mather[2], Joanne M. Morrisey[2], Benjamin A. Garcia[3], Akhil B. Vaidya[2], Joshua D. Rabinowitz[4] & Manuel Llinás[1]

A central hub of carbon metabolism is the tricarboxylic acid cycle[1], which serves to connect the processes of glycolysis, gluconeogenesis, respiration, amino acid synthesis and other biosynthetic pathways. The protozoan intracellular malaria parasites (*Plasmodium* spp.), however, have long been suspected of possessing a significantly streamlined carbon metabolic network in which tricarboxylic acid metabolism plays a minor role[2]. Blood-stage *Plasmodium* parasites rely almost entirely on glucose fermentation for energy and consume minimal amounts of oxygen[3], yet the parasite genome encodes all of the enzymes necessary for a complete tricarboxylic acid cycle[4]. Here, by tracing ^{13}C-labelled compounds using mass spectrometry[5], we show that tricarboxylic acid metabolism in the human malaria parasite *Plasmodium falciparum* is largely disconnected from glycolysis and is organized along a fundamentally different architecture from the canonical textbook pathway. We find that this pathway is not cyclic, but rather is a branched structure in which the major carbon sources are the amino acids glutamate and glutamine. As a consequence of this branched architecture, several reactions must run in the reverse of the standard direction, thereby generating two-carbon units in the form of acetyl-coenzyme A. We further show that glutamine-derived acetyl-coenzyme A is used for histone acetylation, whereas glucose-derived acetyl-coenzyme A is used to acetylate amino sugars. Thus, the parasite has evolved two independent production mechanisms for acetyl-coenzyme A with different biological functions. These results significantly clarify our understanding of the *Plasmodium* metabolic network and highlight the ability of altered variants of central carbon metabolism to arise in response to unique environments.

The mitochondrion of *P. falciparum* contains the smallest genome sequenced to date, and seems to have evolved reduced functional roles compared with other eukaryotic organisms[6]. Moreover, the limited number of mitochondrial cristae, minimal oxygen consumption and rapid fermentation of glucose into lactate that are observed in intraerythrocytic human malaria parasites suggest that oxidative phosphorylation is not a significant source of ATP-generation during the blood stage[6]. Blood-stage *Plasmodium spp.* have also dispensed with several of the functions often associated with the mitochondrial tricarboxylic acid (TCA) cycle, such as *de novo* amino acid biosynthesis. Although the parasite possesses a functional electron-transport chain, and mitochondrial membrane potential is required for survival, we have shown that the critical metabolic function of electron transport during blood-stage growth is the regeneration of ubiquinone to supply pyrimidine biosynthesis[7].

Several lines of evidence, however, suggest that TCA metabolism plays an active role in the metabolism of the parasite. The parasite genome encodes orthologues for all TCA cycle enzymes[4], which are all transcribed during the blood stage[8]. The citrate synthase orthologue (PF10_0218), aconitase (PF13_0229) and isocitrate dehydrogenase (PfIDH, PF13_0242, see Supplementary Discussion) have been localized to the mitochondrion[9,10], and PfIDH, aconitase and succinate dehydrogenase complex (PFL0630w, PF10_0334) have been biochemically characterized[10–12], suggesting an active mitochondrial pathway. The presence of an essential *de novo* haem biosynthesis pathway in *P. falciparum*[2] further implies that succinyl-coenzyme A (succinyl-CoA) must be generated in the mitochondrion. We have found that the intracellular levels of several TCA metabolites oscillate over the parasite growth cycle roughly in phase with the expression profiles of cognate enzymes[13]. Therefore, TCA metabolites are actively synthesized by the parasite. However, the *P. falciparum* pyruvate dehydrogenase (PDH) complex localizes not to the mitochondrion but to the apicoplast, a non-photosynthetic plastid-like organelle[14]. Thus, instead of its canonical role of feeding glucose-derived carbon into the TCA cycle, the suggested role of PDH is solely to produce acetyl-coenzyme A (acetyl-CoA) for fatty acid elongation[14].

In addition to glucose, major TCA cycle carbon sources in many organisms are the amino acids aspartate, asparagine, glutamate and glutamine, which can be deaminated to yield oxaloacetate or 2-oxoglutarate (α-ketoglutarate). To elucidate the role of the TCA cycle in parasite metabolism, we have determined the major carbon source contributing to the accumulation of TCA intermediates. By culturing synchronized parasite-infected red blood cells in medium supplemented with U-^{13}C-glucose, U-^{13}C-^{15}N-aspartate or U-^{13}C-^{15}N-glutamine, where U indicates labelling at all carbon or nitrogen atoms, we measured intracellular metabolite isotope-labelling patterns throughout the 48-hour parasite cell cycle using a liquid chromatography–mass spectrometry (LC–MS) platform capable of detecting most central carbon metabolites.

As expected, in parasites grown on U-^{13}C-glucose the pools of all glycolytic intermediates were rapidly and uniformly labelled (data not shown). We observed limited labelling of carboxylic acid pools, with moderate amounts of +3 ^{13}C-malate and +3 ^{13}C-fumarate, where +3 indicates labelling at three carbon atoms. These +3 forms are consistent with phosphoenolpyruvate (PEP) carboxylation incorporating unlabelled carbonate from the gaseous environment[15] (Fig. 1a). The absence of labelling in other TCA intermediates suggests that these labelled dicarboxylic acids derive from cytosolic pathways independent of mitochondrial TCA metabolism (Supplementary Fig. 1a). Similarly, parasite growth on U-^{13}C-^{15}N-aspartate results only in the generation of +4 ^{13}C-malate and +4 ^{13}C-fumarate (Supplementary Fig. 2), which can also occur in the cytosol (Supplementary Fig. 1b).

When parasites are fed U-^{13}C-glucose, PDH-complex activity yields acetyl-labelled ^{13}C-acetyl-CoA (Fig. 2a). Feeding on labelled

[1]Department of Molecular Biology and Lewis-Sigler Institute for Integrative Genomics, Princeton University, Princeton, New Jersey 08544, USA. [2]Center for Molecular Parasitology, Drexel University College of Medicine, Philadelphia, Pennsylvania 19129, USA. [3]Department of Molecular Biology, Princeton University, Princeton, New Jersey 08544, USA. [4]Department of Chemistry and Lewis-Sigler Institute for Integrative Genomics, Princeton University, Princeton, New Jersey 08544, USA.

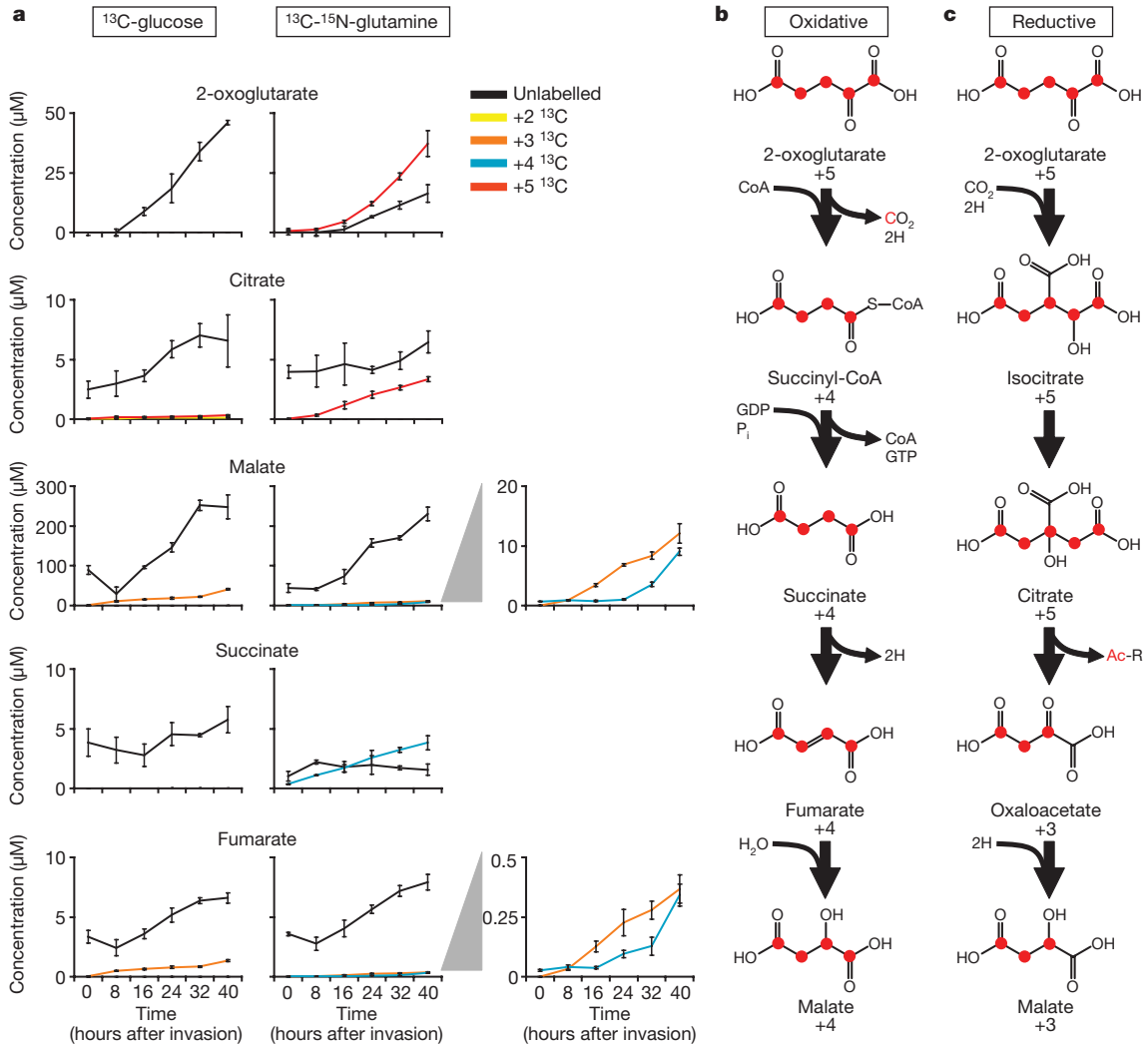

Figure 1 | Glutamine drives reverse flux through the TCA cycle. **a**, Concentrations of different isotope-labelled carboxylic acids in extracts of *P. falciparum*-infected red blood cells. We cultured synchronized parasites in medium supplemented with either U-^{13}C-glucose or U-^{13}C-^{15}N-glutamine 2 h before invasion, then extracted them every 8 hours after invasion for high-performance LC–MS (HPLC–MS) analysis. The plots to the right of the grey triangles zoom in on the profiles of the labelled metabolites. The +3 and +4 malate arises from the reductive and oxidative pathways, respectively, whereas +3 fumarate probably derives from interconversion of fumarate and malate by fumarate hydratase (PFI1340w). Error bars show the s.d. of $n = 3$ biological replicates. **b**, Schematic of the oxidative pathway from 2-oxoglutarate to malate. Red dots denote ^{13}C atoms arising from U-^{13}C-^{15}N-glutamine. GDP, guanosine diphosphate; GTP, guanosine triphosphate; P_i, inorganic phosphate. **c**, Schematic of the reductive carboxylation pathway from 2-oxoglutarate to malate. Ac-R represents either acetyl-CoA or acetate.

glucose results in labelling of only a small fraction of the total acetyl-CoA pool, suggesting the presence of additional sources of two-carbon units. U-^{13}C-glucose feeding also results in small but measurable amounts of both +2 and +5 ^{13}C-citrate (Fig. 1a), which derive from the condensation of acetyl-labelled ^{13}C-acetyl-CoA with either unlabelled oxaloacetate or +3 ^{13}C-oxaloacetate, respectively. These labelled forms account for only a minor fraction of citrate, and the labelling does not propagate to other intermediates downstream in the TCA cycle. These data raised the possibility that glucose- and aspartate-derived metabolites are disconnected from mitochondrial TCA metabolism.

Consistent with the TCA cycle being fed instead from glutamine, we find significant labelling of all TCA compounds in parasites grown in the presence of U-^{13}C-^{15}N-glutamine (Fig. 1a). Extracellular glutamine is rapidly taken up by parasitized red blood cells[16] and deamidated to glutamate, which can donate its carbon skeleton to TCA metabolism through conversion to 2-oxoglutarate. Although the growth medium contains only labelled glutamine, the intracellular glutamine/glutamate pools are incompletely labelled owing to the generation of unlabelled amino acids by haemoglobin catabolism[17]. Consistent with this glutamine-driven reaction pathway, 2-oxoglutarate is labelled at all five carbons (Fig. 1a). We also observe the +4 ^{13}C-labelled forms of the four-carbon (C4) compounds succinate, fumarate and malate, expected from the canonical TCA cycle reactions occurring in the standard clockwise direction (Fig. 1b).

We detect only +5 ^{13}C forms of the C6 metabolite citrate. This labelling is inconsistent with the TCA cycle turning in the standard clockwise direction, but is characteristic of the reductive carboxylation of 2-oxoglutarate to isocitrate, followed by isomerization to citrate[18], in the reverse of standard TCA cycle directionality (Fig. 1c). We also observe +3 ^{13}C-labelled forms of both malate and fumarate, which are generated with temporal profiles similar to those of +5 ^{13}C-citrate (Fig. 1a). Such malate labelling is consistent with +5 ^{13}C-citrate being cleaved into +2 ^{13}C-acetate or acetyl-CoA and +3 ^{13}C-oxaloacetate, which is then reduced to +3 ^{13}C-malate (Fig. 1c). We also observe +2 ^{13}C-acetyl-CoA during growth on U-^{13}C-^{15}N-glutamine (Fig. 2a). Thus several TCA cycle reactions are running with net flux in the reverse direction, in the process generating C2 units from 2-oxoglutarate via citrate.

To further dissect the biological role of this reverse-TCA branch, we investigated the major metabolic fates for C2 units: fatty acid synthesis, protein modification and small-molecule acetylation. We

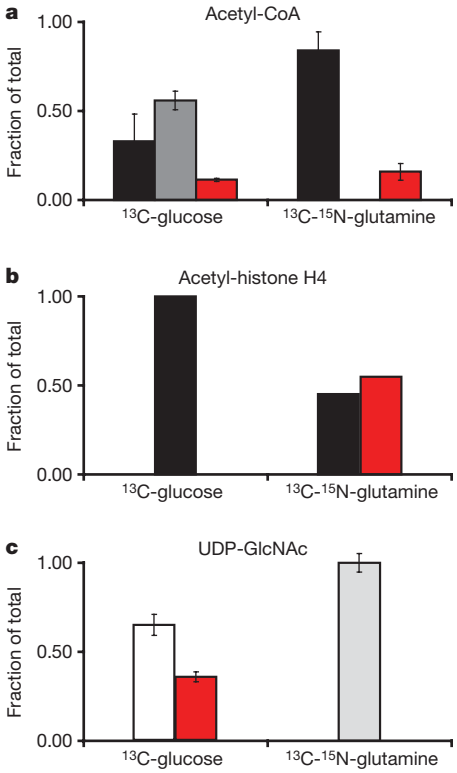

Figure 2 | Acetyl groups deriving from glucose and glutamine are functionally distinct. **a**, Labelling of acetyl-CoA in extracts of *P. falciparum*-infected red blood cells at $t = 40$ hours after invasion as determined by HPLC–MS. **b**, Labelling of a singly acetylated peptide derived from the N-terminal tail of histone H4, determined by proteomic mass spectrometry. **c**, Labelling of UDP-GlcNAc at $t = 40$ hours after invasion. Black bars, unlabelled molecule; red bars, the molecule labelled at both carbons of the acetyl group, regardless of any other labelling; dark grey bars, acetyl-CoA labelled at all five carbons of the ribose moiety of CoA, but not the acetyl group; white bars, UDP-GlcNAc labelled at some combination of the glucose, ribose or pyrimidine ring, but not the acetyl group; light grey bars, UDP-GlcNAc labelled at 0–3 nitrogens, but at no carbons. Error bars show the s.d. of $n = 3$ biological replicates.

profiled ^{13}C labelling of parasite lipids during growth on U-^{13}C-glucose or U-^{13}C-^{15}N-glutamine by gas chromatography–mass spectrometry (GC–MS) but were unable to detect labelling under either condition, which is consistent with recent reports that the parasite's *de novo* fatty acid synthesis pathway is not required during the blood stages[19,20]. Some of the major protein-acetylation targets in eukaryotes are the lysine residues within the amino-terminal tails of histones. When parasites are cultured in medium containing either U-^{13}C-glucose or U-^{13}C-^{15}N-glutamine, we observe robust labelling of the acetyl groups in histone tails only in the U-^{13}C-^{15}N-glutamine-fed cultures (Fig. 2b, Supplementary Fig. 3). The acetyl-labelled histones comprise approximately 56% of the total acetylated histone pool, a proportion similar to the fractional labelling of the 2-oxoglutarate pool. However, UDP-N-acetyl-glucosamine (UDP-GlcNAc), a nucleotide amino sugar acetylated in the endoplasmic reticulum during the biosynthesis of glycosylphosphatidylinositol-anchored proteins associated with malaria pathogenesis[21], is labelled at the acetyl group only during growth on U-^{13}C-glucose (Fig. 2c). Thus it appears that the malaria parasite has evolved two independent pathways that produce acetyl-CoA for different metabolic functions. How glucose- and glutamine-derived C2 units are maintained as functionally distinct pools and transported from their respective organelles to different sites of acetylation remains to be investigated.

Our metabolic labelling data suggest a branched architecture for mitochondrial carbon metabolism in which both arms produce malate. To achieve a net flux through these pathways it would be necessary to remove this terminal product, either by conversion or excretion. When we analysed the liquid culture media from cultures grown on labelled nutrients, we found that malate, 2-oxoglutarate and, to a lesser extent, fumarate are excreted from infected red blood cells at a significant rate (Fig. 3 and Supplementary Fig. 4). Cytosolic fumarate is a byproduct of the parasite's purine salvage pathway[22], whereas 2-oxoglutarate is produced by glutamate dehydrogenase. Our data imply that these metabolites, as well as malate derived from both cytosolic and mitochondrial pathways, flow out of the system as waste products.

On the basis of these results, we propose a new model for central carbon metabolism in blood-stage *Plasmodium spp.* (Fig. 4). In this pathway the ultimate carbon source for mitochondrial carboxylic acid pools is the amino acids glutamine and glutamate, and carbon flux in the mitochondrion is organized into two independent linear branches. Branch 1 (red in Fig. 4) begins with the reductive carboxylation of 2-oxoglutarate to isocitrate, which is then isomerized to citrate. This citrate is cleaved into a C2 compound and oxaloacetate, which is reduced to malate. Branch 2 (blue in Fig. 4) comprises the standard clockwise turning of the TCA cycle to oxidize 2-oxoglutarate to malate, in the process generating reducing power and succinyl-CoA, an essential precursor for haem biosynthesis. Two labelled forms are observed for malate and fumarate, but no other TCA intermediates, during growth on U-^{13}C-^{15}N-glutamine, suggesting that both branches converge at these metabolites, which are the terminal products of each. On the basis of current evidence, our model depicts these pathways as mitochondrial, although the localization of some enzymatic steps and details regarding transport are yet to be fully established (see Supplementary Discussion and Supplementary Figs 5–8).

This model for branched TCA metabolism is fundamentally different from any yet described. Reductive flux from 2-oxoglutarate has been demonstrated in human brown adipose cell cultures[18], in which this pathway was shown to be a source of lipogenic C2 units[18]. However, such adipose cells seem capable of running a complete TCA cycle simultaneously with this reductive pathway. This was proposed to be due to the presence of two mitochondrial isoforms of isocitrate

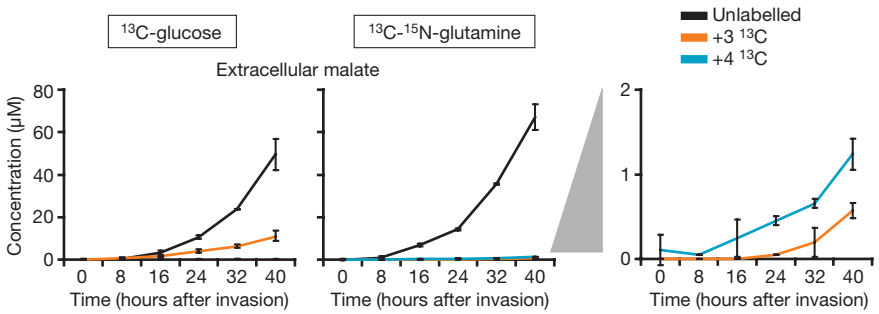

Figure 3 | Malate excretion by *P. falciparum*-infected red blood cell cultures. We grew and cultured parasites as described above, collected samples of the culture medium and analysed them by HPLC–MS. The data are given as molar concentrations in the medium samples. The plot at the right, indicated by grey triangle, is a close up of the profiles of the labelled metabolites. All error bars show the s.d. of $n = 3$ biological replicates.

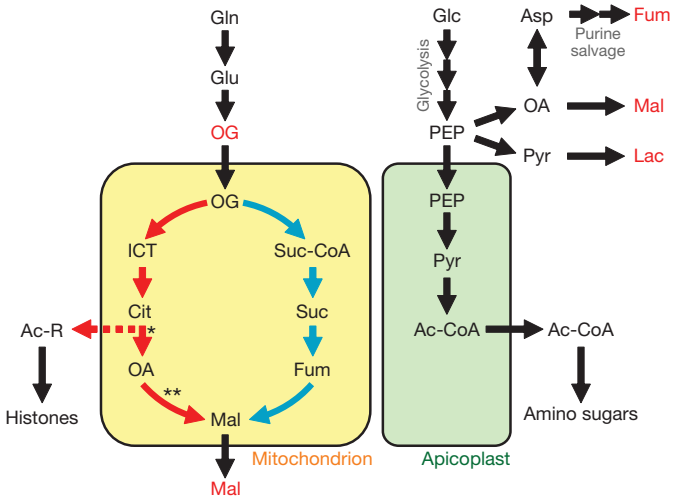

Figure 4 | An integrated model for central carbon metabolism in *P. falciparum*. Arrows show the direction of net flux; multiple arrows depict pathways not shown in their entirety and are labelled as such. Metabolites in red are those found to flow out into the medium as waste products. Red arrows indicate the reductive pathway of TCA metabolism; blue arrows show the oxidative pathway. Asterisk (*), the specific enzyme responsible for the citrate cleavage step and its localization are unclear (see Supplementary Discussion). Double asterisk (**), there are two predicted enzymes capable of catalysing this reaction, the cytosolic malate dehydrogenase (PFF0895w) and the putative mitochondrial malate:quinone oxidoreductase (MAL6P1.258). Abbreviations: Gln, glutamine; Glu, glutamate; OG, 2-oxoglutarate; ICT, isocitrate; Cit, citrate; Ac-R, acetate/acetyl-CoA; Ac-CoA, acetyl-CoA; OA, oxaloacetate; Mal, malate; Suc, succinyl; Suc-CoA, succinyl-CoA; Fum, fumarate; Glc, glucose; Asp, aspartate; PEP, phosphoenolpyruvate; Pyr, pyruvate; Lac, lactate.

dehydrogenase (IDH) in the human cells: IDH3, the canonical TCA-cycle enzyme which uses NAD(H) as a cofactor, and IDH2, which is specific for NADP(H) and may run in the reductive direction owing to a mitochondrial $NADP^+$:NADPH ratio favouring the reverse reaction[18]. The *P. falciparum* genome encodes only an NADP(H)-specific, mitochondrial IDH[11], suggesting that it may have entirely lost the ability to run a textbook TCA cycle and is effectively locked into this branched architecture. We propose that the mitochondrial NADPH required by this reductive pathway may be generated by the parasite's NADP(H)-specific glutamate dehydrogenase (PF14_0164), and glutamate oxidation has been detected in isolated *P. falciparum* mitochondria[23].

This branched TCA pathway can be understood as an evolutionary trade-off in which metabolic flexibility is lost to optimize growth within the specific environment of the host cell. Within the human bloodstream, an abundant and homeostatic supply of glucose ensures a constant supply of energy, whereas the high levels of plasma glutamine (about 0.5 mM) represent a ready source of C5 carbon skeletons to drive the mitochondrial production of reduced ubiquinone, succinyl-CoA and C2 acetyl units. In human cells, production of nuclear acetyl-CoA from mitochondrially derived citrate is a major determinant of the acetylation state of histones[24], and acetylation of metabolic enzymes is gaining recognition as a major post-translational modification involved in sensing and regulating responses to nutrient availability in diverse organisms[25,26]. It is possible that flux through this reductive TCA pathway in *P. falciparum* serves as a nutrient sensor regulating enzymatic activities and transcriptional responses by means of protein acetylation. Also, studies have found that TCA cycle enzymes are upregulated in a subset of patient-derived blood-stage parasite isolates[27] as well as in salivary gland sporozoites[27,28]. Our results suggest that under these glucose-limited conditions, reductive TCA flux might compensate for reduced synthesis of C2 units from glucose. Whether the pathway architecture described in our model is maintained within other tissues invaded during the parasite life cycle, such as the mosquito midgut and salivary gland or the human liver, merits further study, because the nutrient availabilities and metabolic demands in these environments vary substantially.

Our results highlight the growing part that metabolomic technologies play in elucidating the architecture of metabolic pathways, particularly in such divergent pathogens as *Apicomplexan* parasites. Genomic reconstructions[4], which generally map metabolic networks onto those of well-studied model organisms, must be informed by direct experimental evidence or run the risk of failing to identify the pathways that represent the best candidates for drug targets. This study clarifies our understanding of the metabolism underlying plasmodial mitochondrial electron flow, haem biosynthesis and histone acetylation, all of which are current or suggested targets for pharmaceutical intervention[29,30]. In addition, it presents a clear case in which a fundamental metabolic pathway has undergone significant evolutionary adaptation towards a particular environmental niche.

METHODS SUMMARY

We performed *P. falciparum* culturing and metabolomics essentially as described[13]. For further details, and for descriptions of cloning, fluorescent imaging, mitochondrial isolation, enzyme assays, histone extraction, proteomics and GC–MS analysis, see the Supplementary Methods.

Full Methods and any associated references are available in the online version of the paper at www.nature.com/nature.

Received 19 March; accepted 11 June 2010.

1. Krebs, H. A. & Johnson, W. A. The role of citric acid in intermediate metabolism in animal tissues. *Enzymologia* **4,** 148–156 (1937).
2. van Dooren, G. G., Stimmler, L. M. & McFadden, G. I. Metabolic maps and functions of the *Plasmodium* mitochondrion. *FEMS Microbiol. Rev.* **30,** 596–630 (2006).
3. Sherman, I. W. in *Malaria, Parasite Biology, Pathogenesis and Protection* (ed. Sherman, I. W.) 135–143 (ASM, 1998).
4. Gardner, M. J. *et al.* Genome sequence of the human malaria parasite *Plasmodium falciparum*. *Nature* **419,** 498–511 (2002).
5. Munger, J. *et al.* Systems-level metabolic flux profiling identifies fatty acid synthesis as a target for antiviral therapy. *Nature Biotechnol.* **26,** 1179–1186 (2008).
6. Vaidya, A. B. & Mather, M. W. Mitochondrial evolution and functions in malaria parasites. *Annu. Rev. Microbiol.* **63,** 249–267 (2009).
7. Painter, H. J., Morrisey, J. M., Mather, M. W. & Vaidya, A. B. Specific role of mitochondrial electron transport in blood-stage *Plasmodium falciparum*. *Nature* **446,** 88–91 (2007).
8. Bozdech, Z. *et al.* The transcriptome of the intraerythrocytic developmental cycle of *Plasmodium falciparum*. *PLoS Biol.* **1,** e5 (2003).
9. Tonkin, C. J. *et al.* Localization of organellar proteins in *Plasmodium falciparum* using a novel set of transfection vectors and a new immunofluorescence fixation method. *Mol. Biochem. Parasitol.* **137,** 13–21 (2004).
10. Hodges, M. *et al.* An iron regulatory-like protein expressed in *Plasmodium falciparum* displays aconitase activity. *Mol. Biochem. Parasitol.* **143,** 29–38 (2005).
11. Wrenger, C. & Muller, S. Isocitrate dehydrogenase of *Plasmodium falciparum*. *Eur. J. Biochem.* **270,** 1775–1783 (2003).
12. Suraveratum, N. *et al.* Purification and characterization of *Plasmodium falciparum* succinate dehydrogenase. *Mol. Biochem. Parasitol.* **105,** 215–222 (2000).
13. Olszewski, K. L. *et al.* Host-parasite interactions revealed by *Plasmodium falciparum* metabolomics. *Cell Host Microbe* **5,** 191–199 (2009).
14. Foth, B. J. *et al.* The malaria parasite *Plasmodium falciparum* has only one pyruvate dehydrogenase complex, which is located in the apicoplast. *Mol. Microbiol.* **55,** 39–53 (2005).
15. Blum, J. J. & Ginsburg, H. Absence of α-ketoglutarate dehydrogenase activity and presence of CO_2-fixing activity in *Plasmodium falciparum* grown *in vitro* in human erythrocytes. *J. Protozool.* **31,** 167–169 (1984).
16. Elford, B. C., Haynes, J. D., Chulay, J. D. & Wilson, R. J. Selective stage-specific changes in the permeability to small hydrophilic solutes of human erythrocytes infected with *Plasmodium falciparum*. *Mol. Biochem. Parasitol.* **16,** 43–60 (1985).
17. Liu, J. *et al. Plasmodium falciparum* ensures its amino acid supply with multiple acquisition pathways and redundant proteolytic enzyme systems. *Proc. Natl Acad. Sci. USA* **103,** 8840–8845 (2006).
18. Yoo, H., Antoniewicz, M. R., Stephanopoulos, G. & Kelleher, J. K. Quantifying reductive carboxylation flux of glutamine to lipid in a brown adipocyte cell line. *J. Biol. Chem.* **283,** 20621–20627 (2008).
19. Vaughan, A. M. *et al.* Type II fatty acid synthesis is essential only for malaria parasite late liver stage development. *Cell. Microbiol.* **11,** 506–520 (2009).
20. Yu, M. *et al.* The fatty acid biosynthesis enzyme FabI plays a key role in the development of liver-stage malarial parasites. *Cell Host Microbe* **4,** 567–578 (2008).

21. Gowda, D. C. & Davidson, E. A. Protein glycosylation in the malaria parasite. *Parasitol. Today* **15,** 147–152 (1999).
22. Downie, M. J., Kirk, K. & Mamoun, C. B. Purine salvage pathways in the intraerythrocytic malaria parasite *Plasmodium falciparum*. *Eukaryot. Cell* **7,** 1231–1237 (2008).
23. Fry, M. & Beesley, J. E. Mitochondria of mammalian *Plasmodium spp*. *Parasitology* **102,** 17–26 (1991).
24. Wellen, K. E. *et al.* ATP-citrate lyase links cellular metabolism to histone acetylation. *Science* **324,** 1076–1080 (2009).
25. Wang, Q. *et al.* Acetylation of metabolic enzymes coordinates carbon source utilization and metabolic flux. *Science* **327,** 1004–1007 (2010).
26. Zhao, S. *et al.* Regulation of cellular metabolism by protein lysine acetylation. *Science* **327,** 1000–1004 (2010).
27. Daily, J. P. *et al.* Distinct physiological states of *Plasmodium falciparum* in malaria-infected patients. *Nature* **450,** 1091–1095 (2007).
28. Lasonder, E. *et al.* Proteomic profiling of *Plasmodium* sporozoite maturation identifies new proteins essential for parasite development and infectivity. *PLoS Pathog.* **4,** e1000195 (2008).
29. Mather, M. W., Henry, K. W. & Vaidya, A. B. Mitochondrial drug targets in apicomplexan parasites. *Curr. Drug Targets* **8,** 49–60 (2007).
30. Andrews, K. T., Tran, T. N., Wheatley, N. C. & Fairlie, D. P. Targeting histone deacetylase inhibitors for anti-malarial therapy. *Curr. Top. Med. Chem.* **9,** 292–308 (2009).

Supplementary Information is linked to the online version of the paper at www.nature.com/nature.

Acknowledgements We thank G. McFadden and I. Sherman for discussions and scrutiny of the manuscript; B. Bennett, T. Campbell, E. De Silva, J. O'Hara, and H. Painter for reading of the manuscript; I. Ying for assistance with histone extraction; T. Spurck and C. Tonkin for the modified erythrocyte immobilization procedure for microscopy; M. Clasquin and W. Lu for developing the LC–MS methodology; E. Melamud for LC–MS data extraction and analysis; and J. Groves and H. Cooper for GC–MS analysis. M.L. is funded by the Burroughs Wellcome Fund and an NIH Director's New Innovators award (1DP2OD001315-01). J.D.R. is funded by a Beckman Young Investigators award, an NSF CAREER award and NIH R01 AI078063. M.L and J.D.R. receive support from the Center for Quantitative Biology (P50 GM071508). B.A.G. receives support from NSF grant CBET-0941143. K.L.O. is funded by an NSF Graduate Research Fellowship. J.M.M., M.W.M. and A.B.V. are supported by grant AI028398 from NIAID, NIH.

Author Contributions K.L.O. cultured the parasites, and collected and analysed all LC–MS and GC–MS data; B.A.G. performed mass spectrometric analysis of histones. M.W.M. and J.M.M. carried out IDH localization studies. M.W.M. purified mitochondria and K.L.O. did biochemical assays. K.L.O., M.L., J.D.R., M.W.M., A.B.V. and B.A.G. designed the study; J.D.R. provided the metabolomic technology. M.L. and K.L.O. wrote the paper. All authors discussed the results and commented on the manuscript.

Author Information Reprints and permissions information is available at www.nature.com/reprints. The authors declare no competing financial interests. Readers are welcome to comment on the online version of this article at www.nature.com/nature. Correspondence and requests for materials should be addressed to M.L. (manuel@genomics.princeton.edu).

METHODS

***P. falciparum* culturing and metabolite extraction.** We maintained and synchronized *P. falciparum* cultures by standard methods[31,32]. Briefly, we grew *P. falciparum*-infected (3D7 strain) red blood cells in RPMI 1640 culture medium supplemented with sodium carbonate (2 mg ml^{-1}), hypoxanthine (100 μM), Albumax II (0.25%) and gentamycin (50 μg ml^{-1}) in a humidified incubator at 5% CO_2, 6% O_2 and 37 °C. We collected human red blood cells used for culturing two days before use, in tubes supplemented with sodium heparin instead of standard citrate-containing anticoagulants to avoid contaminating citrate.

For metabolic labelling experiments, growth medium was formulated according to the standard nutrient concentrations of RPMI 1640 medium[33]. We supplied vitamins using RPMI 100X Vitamins Solution (Sigma-Aldrich); we purchased inorganic salts and all other nutrients individually from Sigma-Aldrich; they were of the highest purity available. We found, by standard growth assays, that this reformulated medium was indistinguishable from commercial RPMI 1640 mixes in supporting *P. falciparum* growth. We purchased U-^{13}C-glucose, U-^{13}C-^{15}N-aspartate and U-^{13}C-^{15}N-glutamine from Cambridge Isotope Laboratories and used them to replace the replace the unlabelled nutrient at the normal concentrations of each (glucose, 2 g l^{-1}; aspartate, 20 mg l^{-1}; glutamine, 300 mg l^{-1}).

We carried out metabolic labelling experiments as follows: we inspected a highly synchronized *P. falciparum* culture in the late schizont stage hourly by microscope until host-cell lysis and reinvasion was complete. We then adjusted this culture to 6% parasitaemia using cultured red blood cells, diluted it to 0.4% haematocrit in fresh, prewarmed (37 °C) medium containing one of the labelled nutrients, and returned it to the incubator. We allowed the cultures to equilibrate for 2 h and then collected infected red blood cells and culture media for the $t = 0$ time point and at 8-h intervals thereafter. We similarly treated an uninfected red blood cell culture and it extracted at $t = 0$ to use for normalization.

We extracted the metabolite using a modified version of our previous protocol[13]. Briefly, we pelleted red blood cells from liquid cultures by centrifugation for 5 min at 500*g*. We collected medium samples from the supernatant by dilution in 4 volumes of 100% methanol at −70 °C, then removed the supernatant by aspiration. We flash-quenched the cell pellet was in 4 volumes of 100% methanol at −70 °C and incubated it on dry ice for 15 min, with vortexing every 5 min. We centrifuged the lysate for 5 min at 500*g* and collected the supernatant. We re-extracted the pellet in 10 volumes of 80:10 methanol:water at 4 °C and agitated it with ultrasound on ice in a water-bath sonicator for 15 min. We then centrifuged it for 5 min at 16,000*g* and collected the supernatant, then pooled it with the previous extract. We centrifuged the pooled extract for 10 min at 16,000*g* to precipitate denatured protein, and then transferred the supernatant to a fresh tube and dried it under nitrogen flow. We stored the dried extracts at −70 °C until we analysed them by LC–MS (less than 96 h). For analysis, we resuspended the dried extracts in 200 μl of chromatographic buffer A (97:3 water:methanol, 10 mM tributylamine, 15 mM acetic acid). We also prepared medium extracts described above. To quantitate TCA intermediates in medium and cell extracts, we maintained a parasite culture in label-free medium and extracted it at 24 h post-invasion into methanol-containing isotope-labelled internal standards at the following concentrations: U-^{13}C-malic acid, 5 μg ml^{-1}; U-^{13}C-fumaric acid, 0.5 μg ml^{-1}; 1,4-^{13}C-succinic acid, 0.5 μg ml^{-1}; 2,4-^{13}C-citric acid, 1 μg ml^{-1}; 1,2,3,4-^{13}C-ketoglutaric acid disodium, 5 μg ml^{-1} (Cambridge Isotope Laboratories). We otherwise performed the extraction as above.

LC–MS instrumentation. We did LC–MS analyses on a Exactive Orbitrap mass spectrometer, coupled with an Accela U-HPLC system (Thermo Fisher Scientific) and HTC PAL autosampler (CTC Analytics AG). We achieved liquid chromatography separation on a Synergy Hydro-RP column (100 × 2 mm, 2.5 μ particle size, Phenomenex); the gradient is modified from our previous method[34]: 0 min, 0% B; 2.5 min, 0% B; 5 min, 20% B; 7.5 min, 20% B; 13 min, 55% B; 15.5 min, 95% B; 18.5 min, 95% B; 19 min, 0% B; 25 min, 0% B. Solvent A is 97:3 water:methanol with 10 mM tributylamine and 15 mM acetic acid; solvent B is methanol. Other LC parameters are: autosampler temperature 4 °C; injection volume 10 μl; column temperature 25 °C.

We operated the Exactive Orbitrap mass spectrometer in negative mode, scanning mass-charge ratio (m/z) 85–1,000. Other instrumental parameters are: resolution 100,000 at 1 Hz (1 scan per second); AGC (automatic gain control) target 3E6; maximum injection time 100 μs; sheath gas flow rate 25 (arbitrary unit); aux gas flow rate 8 (arbitrary unit); sweep gas flow rate 3 (arbitrary unit); spray voltage 3 kV; capillary temperature 270 °C; capillary voltage −50 V; tube lens voltage −100 V.

LC–MS data extraction and analysis. We converted Thermo Fisher mass spectrometry RAW files from profile mode into centroid mode using the ReAdW program[35]. We loaded centroide-mode files into MAVEN, an in-house analysis program, and aligned them with a nonlinear regression using a high degree polynomial to the retention times of the highest-intensity m/z measurements from each sample to construct a median reference. We extracted ion chromatograms using a 5-p.p.m. window centred around the expected m/z of each compound and smoothed by applying a Gaussian filter to the intensity signal. Within each extracted ion chromatogram, we detected peaks and evaluated their quality using a neural-network-based classification model that takes into account peak height, peak width, peak area, the signal to noise ratio and the peak shape[36]. We grouped peaks across samples and matched them to the expected retention time of each compound. We used the peak closest to the expected retention with a quality score of more than 0.5 for quantitation. We hand-checked all peaks used for quantitation after automated extraction and assignment. We extracted the isotopically labelled forms of compounds in a similar manner. We based the quantitation of labelled forms on the highest-intensity peak within a 5-p.p.m. window around the expected m/z of the ^{13}C- and/or ^{15}N-labelled form of the compound. We will describe the specifics of the MAVEN program in a forthcoming publication.

We identified metabolites on the basis of both their match to the expected m/z ratio and their chromatographic retention times determined previously for standard solutions. We identified isotope-labelled forms using the expected mass shifts given by ^{13}C and ^{15}N. Where ambiguous, we determined the positional labelling of specific atoms within the molecule by LC–MS or MS analysis as described previously[13]. We used the height of the extracted peak for each compound as the signal. We corrected the raw signals for each labelled form to account for the naturally occurring isotope distribution as calculated by the Qual Browser included in the Xcalibur software suite (Thermo Fisher Scientific). We added the signal from naturally occurring isotopes to the signal of the unlabelled form. Similarly, we discounted signals that were due to incomplete labelling of the isotope-labelled nutrients (which are generally 98–99% fully labelled). For quantitation experiments, we determined the signal ratio of the unlabelled metabolite to its isotope-labelled internal standard and used it to calculate the concentration of the metabolite in the extract at the 24-h time point. We used the relative signal in the other time-point samples to calculate the concentrations over the temporal profile.

We treated signals from the uninfected red blood cell sample as the background level in host cells and subtracted them from every time point; where this reduced signals to less than 1,000 counts the signal was set to 1,000 counts, the approximate limit of quantitation for the instrument. Each plotted point shows the average of $n = 3$ biological replicates; error bars show the standard deviation. We plotted the labelled forms only if the average signal in at least one time point is greater than 1,000 counts and the signal represents at least 1% of the signal of the unlabelled form.

Fatty-acid extraction and analysis. For lipid-labelling experiments, we cultured parasites collected at the trophozoite stage as described above, in labelled nutrient-supplemented RPMI media for 96 h (encompassing two growth cycles). We conducted these experiments using normally formulated RPMI and a minimal fatty-acid formulation (lacking Albumax II, we supplemented it with 60 μM lipid-free bovine serum albumin and 30 μM each of myristic, stearic and oleic acids) prepared according to an earlier report that growth in this medium resulted in enhanced elongation of preformed fatty acids by the parasite[37]. We lysed infected red blood cells by treatment with 100 pellet volumes of 0.1% saponin in phosphate-buffered saline (PBS) buffer and collected the freed parasite cells by centrifugation at 2,500*g*, 4 °C for 10 min. After washing the parasite pellet in PBS, we extracted the and derivatized them to fatty acid methyl esters using the protocol of ref. [18].

We investigated the fatty acid methyl esters by GC–MS, using an Agilent 7890A GC coupled to a 5975C inert MSD with an Rtx-5Sil MS (30 m length, 0.25 mm internal diameter, 0.25 μm film) column. We used the thermal gradient: start at 70 °C, holding for 2 min; ramping to 230 °C at 20 °C min^{-1}. We examined the mass spectra of the molecular ions of the palmitic and stearic acid methyl esters (monoisotopic $m/z = 270.45$ and $m/z = 298.51$) for deviation from the naturally occurring isotope distribution indicating ^{13}C incorporation. We detected no incorporation in either the normal or minimal fatty acid RPMI cultures.

Histone extraction and analysis. For histone labelling experiments, we cultured parasites as above in labelled nutrient-supplemented RPMI media for 96 h (encompassing two growth cycles) and collected them at the trophozoite stage. We lysed infected red blood cell cultures (50 ml total volume, 2% haematocrit, 10% parasitaemia) by treatment with 100 pellet volumes of 0.1% saponin in PBS buffer and collected the freed parasite cells by centrifugation at 2,500*g*, 4 °C for 10 min. After washing the parasite pellet in PBS, we acid-extracted[38] and purified[39] the histones according to modified versions of the published protocols. Briefly, we resuspended the parasite pellet in 800 μl of acid-extraction buffer (0.2 M HCl, 1 mM dithiothreitol, 1 mM sodium orthovanadate, 10 mM sodium butyrate, 1 Roche EDTA-free protease inhibitor tablet per 50 ml). We gently agitated the suspension at 4 °C for 2 h, and then centrifuged it at 16,000*g* for

1 min at 4 °C. We collected the supernatant and slowly added 246 µl of 100% trichloroacetic acid. We mixed this by inversion and incubated it on ice overnight, and then centrifuged it at 16,000*g* for 10 min at 4 °C. We discarded the supernatant and washed the pellet twice with cold acetone at 4 °C. We allowed the acetone to evaporate and resuspended the pellet in deionized water for analysis.

We fractionated histone extracts by reverse phase HPLC on a C18 column using 30–60% buffer B in 100 min gradient (buffer A is 5% acetonitrile in 0.2% trifluoroacetic acid (TFA), buffer B is 90% acetonitrile in 0.188% TFA). We pooled fractions containing histone H4 and propionylated them as previously published[40]. We digested propionylated histone H4 with trypsin at a 20:1 protein:enzyme ratio for 7 h at 37 °C. We subjected digested histone H4 to MS analysis on an Orbitrap mass spectrometer, operated by obtaining a full mass spectrum at 30,000 resolution in the Orbitrap followed by 7 data-dependent MS/MS spectra acquired in the ion trap. We interpreted all mass spectra manually. We quantitated ^{13}C labelling using the natural isotope distribution of the propionylated acetyl-H4 peptide calculated by the Qual Browser included in the Xcalibur software suite (Thermo Fisher Scientific).

Preparation of *P. falciparum* mitochondria. We sychronized *P. falciparum* cultures twice by treatment with sorbitol as described, and expanded and collected them at 8% parasitaemia in the early trophozoite stage. We prepared fractions substantially enriched in mitochondria using a procedure modified from the method of ref. 41. We collected parasitized erythrocytes by centrifugation, washed them in AIM medium (120 mM KCl, 20 mM NaCl, 20 mM glucose; 6 mM HEPES buffer, 6 mM MOPS buffer, 1 mM $MgCl_2$, 0.1 mM EGTA; pH 7.0) and lysed them with 0.05% (w/v) saponin in AIM medium. After washing 3 times with AIM medium and once with MSEH buffer (225 mM mannitol, 75 mM sucrose, 4.3 mM $MgCl_2$, 0.25 mM EGTA, 10 mM HEPES (Tris) buffer, 5 mM HEPES (KOH) buffer; pH 7.4), we disrupted the parasites by N_2 cavitation (using a 4639 Cell Disruption Bomb, Parr) at 1,000 p.s.i. (6.9 MPa) for 20 min at 4 °C in de-aerated MSEH buffer containing 5 mM glucose and mitochondrial substrates (5 mM α-glycerophosphate and 2.5 mM dihydroorotate) in the presence of 1 mM PMSF inhibitor and 1 µl of fungal protease inhibitor cocktail (Sigma-Aldrich) per ml. After drop-wise release from the N_2 bomb, we mixed another aliquot of protease inhibitors into the disrupted parasite sample. We removed the unbroken cells and cell debris by centrifugation at 900*g* for 6 min at 4 °C. We passed the low-speed supernatant slowly through a MACS CS column prewashed with MSEH buffer in a Vario MACS magnetic separation apparatus (Miltenyi Biotec) to remove most of the haemozoin from the preparation. We then recovered the mitochondria as a pellet by centrifugation at 23,000*g* for 20 min at 4 °C. We suspended the pellet in a minimal volume of MSEH buffer containing 1 mM dihydroorotate and 1 mg ml^{-1} fatty acid-free BSA and stored at −80 °C.

Mitochondrial IDH assay. We assayed for mitochondrial reductive IDH activity using a modified version of the protocol of ref. 42. Briefly, we thawed purified mitochondrial preparations on ice and diluted them into 9 volumes of assay buffer (final concentration: 50 mM Na_2HPO_4, 0.5 mM $MgCl_2$, 5 mM $NaHCO_3$, 0.2 mM NADPH, 10 mM 1,2,3,4-^{13}C-2-oxoglutarate; pH 7.0) in a sealed tube. We incubated the reaction mixture in a water bath at 37 °C and removed the samples at the specified times. We quenched the reaction by dilution into 9 volumes of methanol at −70 °C. We centrifuged these samples for 15 min at 16,000*g*, 4 °C to precipitate protein and biological material, then we diluted the supernatant was diluted into 9 volumes of water and subjected it to HPLC–MS analysis as described.

Citrate lyase assays. We assayed for ATP:citrate lyase and ATP-independent citrate lyase on lysates of uninfected erythrocytes, infected erythrocytes (trophozoite-stage, 10% parasitaemia), host cell-free parasites (trophozoite-stage) and isolated mitochondria. We prepared host cell-free parasites by standard saponin treatment: briefly, we collected blood cultures by centrifugation (500 *g*, 5 min); washed them once with PBS buffer (500*g*, 5 min); resuspended them at 2% haematocrit in 0.1% w/v saponin in PBS buffer and incubated them for 2 min at 25 °C pelleted them by centrifugation (2,000*g*, 10 min, 4 °C); and washed them once more in PBS buffer (2,000*g*, 10 min, 4 °C).

We performed ATP:citrate lyase assays using a protocol modified slightly from ref. 43. We diluted erythrocyte and parasite cell samples into 9 volumes of lysis buffer (50 mM Tris-HCl buffer (pH 8.0), 50 mM NaCl, 2 mM DTT redox reagent, 1 mM $MgCl_2$, 1 EDTA-free protease inhibitor cocktail tablet per 10 ml; Roche complete Mini), lysed them by three rounds of freeze-thaw cycles (1 min in liquid nitrogen, 5 min in 37 °C water bath) and centrifuged them (16,000*g*, 10 min, 4 °C) to clear the supernatant. We diluted mitochondrial preparations into the same buffer, but with 0.05% dodecyl maltoside to permeabilize the membranes, and lyse them. We diluted 2.5 µl of these samples into 17.5 µl of reaction cocktail with final concentrations of: 87 mM Tris-HCl buffer (pH 8.0), 20 µM $MgCl_2$, 10 mM KCl, 10 mM DTT redox reagent, 100 µM coenzyme A, 150 µM 2,4-^{13}C-citric acid, with or without 400 µM ATP. We incubated the reaction mix for 15 min at 37 °C and terminated the reaction by adding 80 µl of methanol and cooling it to −70 °C on dry ice for 15 min. We centrifuged the samples (16,000*g*, 10 min, 4 °C), diluted the supernatant 1:10 in water and analysed by LC–MS for the production of +1 ^{13}C-acetyl-CoA.

We performed ATP-independent citrate lyase using a protocol modified from ref. 44. We prepared the samples as described above, except in a buffer with the formulation: 10 mM triethanolamine (pH 7.6), 0.3 mM $ZnCl_2$, 454 mM ammonium sulphate, 10 mM DTT redox reagent and 1 EDTA-free protease inhibitor cocktail tablet per 10 ml (Roche complete Mini). We diluted 1 µl of sample into 29 µl of a reaction cocktail to final concentrations: 96 mM triethanolamine (pH 7.6), 0.5 mM $ZnCl_2$, 0.23 mM β-NADH, 0.67 mM 2,4-^{13}C-citric acid, 15 mM ammonium sulphate, 100 units L-lactate dehydrogenase, 50 units malate dehydrogenase. We incubated the reaction mix for 2 h at 37 °C and terminated the reaction by adding 120 µl of methanol and cooling to -70 °C on dry ice for 15 min. We centrifuged the samples (16,000*g*, 10 min, 4 °C) and diluted the supernatant 1:10 in water and analysed it by LC–MS for the enzyme-linked production of +1 ^{13}C-malate and +1 ^{13}C-lactate.

IDH leader-GFP localization. We amplified the GFP gene from pHDGFP (ref. 45) with added 5′ XhoI and 3′ SalI sites. We eliminated the internal BstBI site using site-directed mutagenesis. We sub-cloned the modified GFP into pHHMC*/3R0.5 (ref. 46) digested with XhoI, producing the plasmid pHHGFP19. We amplified the 5′ 204 base pairs (bp) of the Pf IDH gene (PF13_0242), corresponding to the initial 68 amino acids (MGKHIRILKNQYLQFMSKRCIQSKAAFNICGKINVENPIV ELDGDEMTRIIWKDIKEKLILPYVNLKI), from *P. falciparum* 3D7 DNA with primers adding a 5′ BstBI site and a 3′ XhoI site. We inserted the product into pHHGFP19 digested with BstBI and XhoI to produce pHHIDHldrGFP. We confirmed the cloned DNA sequences by sequencing. We transfected *P. falciparum* using standard methods[47] and selected parasites with the drug WR99210.

We used the primers:

GFP–Xhosens, 34-mer: 5′ GCT CTC GAG TCT GCA GCA GCA GCA GCA GCA G 3′.

GFP–Salanti, 50-mer: 5′ GCA GTC GAC TAT TAT AAA TCT TCT TCA GAT ATT AAT TTT TGT TCA GAT CC 3′.

PCR product 806 bp

GFP-rmvBstB-up, 42-mer: 5′ CCA CAC AAT CTG CCC TTT CTA AAG ATC CCA ACG AAA AGA GAG 3′.

GFP-rmvBstB-dn, 42-mer: 5′ CTC TCT TTT CGT TGG GAT CTT TAG AAA GGG CAG ATT GTG TGG 3′.

IDHldr-BstBsens, 42-mer: 5′ GAC GTT CGA ATA AAA TGG GAA AGC ATA TAC GAA TTT TAA AAA 3′.

IDHldr-Xhoanti, 45-mer: 5′ GAT CTC GAG TAT CTT TAA GTT AAC ATA TGG TAA GAT TAA TTT TTC 3′.

Fluorescence microscopy. We suspended live infected erythrocytes in RPMI medium containing mitotracker Red CM-H2XROS (Molecular Probes) at 50 nM and Hoechst 33342 dye (Sigma) at 1 µg ml^{-1} and incubated them at 37 °C for about 25 min. We immobilized the stained erythrocytes on a microscope coverslip in RPMI medium using a fibrin clot procedure modified from ref. 48. We captured images with an Olympus BX60 microscope equipped with a SPOT RT Slider digital camera and software system (Diagnostic Instruments).

31. Trager, W. & Jensen, J. B. Human malaria parasites in continuous culture. *Science* **193,** 673–675 (1976).
32. Lambros, C. & Vanderberg, J. P. Synchronization of *Plasmodium falciparum* erythrocytic stages in culture. *J. Parasitol.* **65,** 418–420 (1979).
33. Moore, G. E., Gerner, R. E. & Franklin, H. A. Culture of normal human leukocytes. *J. Am. Med. Assoc.* **199,** 519–524 (1967).
34. Lu, W., Bennett, B. D. & Rabinowitz, J. D. Analytical strategies for LC–MS-based targeted metabolomics. *J. Chromatogr. B* **871,** 236–242 (2008).
35. Keller, A. *et al.* A uniform proteomics MS/MS analysis platform utilizing open XML file formats. *Mol. Syst. Biol.* **1,** 2005.0017 (2005).
36. Breiman, L. Random forests. *Mach. Learn.* **45,** 5–32 (2001).
37. Mi-Ichi, F., Kita, K. & Mitamura, T. Intraerythrocytic *Plasmodium falciparum* utilize a broad range of serum-derived fatty acids with limited modification for their growth. *Parasitology* **133,** 399–410 (2006).
38. Miao, J., Fan, Q., Cui, L. & Li, J. The malaria parasite *Plasmodium falciparum* histones: organization, expression, and acetylation. *Gene* **369,** 53–65 (2006).
39. Shechter, D., Dormann, H. L., Allis, C. D. & Hake, S. B. Extraction, purification and analysis of histones. *Nature Protocols* **2,** 1445–1457 (2007).
40. Garcia, B. A. *et al.* Chemical derivatization of histones for facilitated analysis by mass spectrometry. *Nature Protocols* **2,** 933–938 (2007).
41. Takashima, E. *et al.* Isolation of mitochondria from *Plasmodium falciparum* showing dihydroorotate dependent respiration. *Parasitol. Int.* **50,** 273–278 (2001).
42. Kornberg, A. & Pricer, W. E. Jr. Di- and triphosphopyridine nucleotide isocitric dehydrogenases in yeast. *J. Biol. Chem.* **189,** 123–136 (1951).
43. Ma, Z., Chu, C. H. & Cheng, D. A novel direct homogeneous assay for ATP citrate lyase. *J. Lipid Res.* **50,** 2131–2135 (2009).
44. Bergmeyer, H. U., Gawehn, K. & Grassl, M. in *Methods of Enzymatic Analysis* Vol. 1 (ed. Bergmeyer, H. U.) 442–443 (Academic, 1974).

45. Kadekoppala, M., Kline, K., Akompong, T. & Haldar, K. Stable expression of a new chimeric fluorescent reporter in the human malaria parasite *Plasmodium falciparum*. *Infect. Immun.* **68,** 2328–2332 (2000).
46. O'Donnell, R. A. *et al.* A genetic screen for improved plasmid segregation reveals a role for Rep20 in the interaction of *Plasmodium falciparum* chromosomes. *EMBO J.* **21,** 1231–1239 (2002).
47. Fidock, D. A. & Wellems, T. E. Transformation with human dihydrofolate reductase renders malaria parasites insensitive to WR99210 but does not affect the intrinsic activity of proguanil. *Proc. Natl Acad. Sci. USA* **94,** 10931–10936 (1997).
48. Forer, A. & Pickett-Heaps, J. D. Cytochalasin D and latrunculin affect chromosome behaviour during meiosis in crane-fly spermatocytes. *Chromosome Res.* **6,** 533–549 (1998).